MICROWAVE-INDUCED ARCING IN FILTERS

S. L. Kaplan, A. A. Cuneo, and R. V. Garver

HARRY DIAMOND LABORATORIES, Adelphi, Md. 20783

ABSTRACT

In a study of the high-power response (particularly arcing) of microwave/RF filters to microwave energy, experiments were performed with a network analyzer and with two 1-MW pulsed sources (S- and X-band). Computer modeling was used to obtain wideband information for parallel coupled-stripline filters during breakdown.

INTRODUCTION

Filters are often used used to prevent undesired RF energy from penetrating into a system where it can cause upset or damage. Arcing between conducting filter elements changes the designed frequency response. Front-end system filters may pass large amounts of energy upon breakdown due to coupling of microwave pulses incident at high power. Experiments have been performed to study the effect of arcing on the isolation of several common filter types. In particular, the series-coupled filter structure appears prone to loss of isolation due to arcing between elements. This structure is characterized by air gaps between series conductors (filters with this structure include the parallel-coupled stripline and capacitive-gap types). The other filters considered are of the lumped-element, stepped-impedance, and interdigital types.

PARALLEL-COUPLED STRIPLINE FILTERS

Parallel-coupled stripline filters are resonant structures consisting of overlapping line-conductors separated by air gaps. A sample of these filters were subjected to high power microwave pulses at S-band and X-band using magnetron sources. These pulses were 1 μs in length, with rise times on the order of 100 ns. The results for five representative filters, denoted F1, F2, F3, F12, and F15, are described here.

According to MacDonald [1], the actual breakdown field, E, in gas is a function of the pressure and the physical dimensions of the filter, which determine the diffusion constant, and the wavelength of the exciting signal. Sharp edges and resonant structures increase field strength and thus the probability of breakdown. The filter substrates have dielectric strengths of about 400 kV/cm, compared to 30 kV/cm for air. Since coupled-line filters have dielectric substrate separating the center elements and the ground planes, breakdown took place only at the air interfaces between the series-coupled elements, near the cornered ends.

Similar patterns of breakdown were observed for each parallel-coupled stripline filter. Figure 1a clearly shows the onset of the breakdown, as increased transmission occurs at the back of the pulse. This characteristic output form has been denoted "tail-blooming." Figure 1b shows a sudden cutoff ("tail-biting") of the transmitted pulse, likely due to the breakdown of a cable connector. Tail-blooming is a sudden decrease in isolation when series arcing occurs. Tail-biting is the abrupt cutoff of transmitted energy when arcing from an

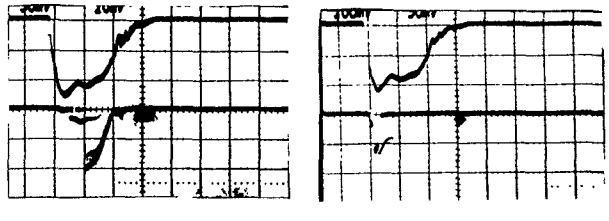

Figure 1 High Power Response of Filter F15

(a) Incident Peak Power of 17 kW (Trans. Power = 17 W)

(b) Incident Peak Power of 43 kW (Trans. Power = 77 W)

0149-645X/88/0000-0811$01.00 © 1988 IEEE

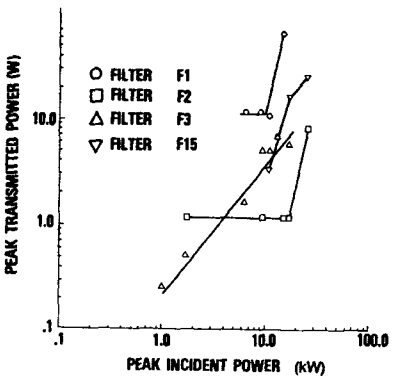

FIGURE 2 Transmitted versus incident peak power for four parallel-coupled-stripline filters, after onset of breakdown, for ~1-μs pulses at 3.28 GHz.

element to ground takes place, as in a typical TR tube response with spike leakage.

Figure 2 shows a graph of peak output power (in watts) versus peak input power (in kilowatts) after the onset of breakdown for four of the parallel-coupled stripline filters. Note that 10-W output power can be obtained for input power as low as 7.5 kW. Also note that for both F1 and F2, the point on the graph where the slope changes is that where tail-blooming starts. For F15 tail-blooming is clearly evident at the first point on the graph.

Two trends associated with the high-power data are evident: both isolation and time before breakdown decrease as input power increases. The lower isolation results from increasing numbers of series arcs at higher input powers. The decreasing delay before breakdown is due to the more rapid buildup of the avalanche charge at the higher electric fields between elements. As breakdown delay decreases, the energy transmitted increases (i.e., the output pulse widens).

A novel technique was employed to precisely locate the arcs in parallel-coupled stripline filters. Small holes (1/32 in. diameter) were drilled through the top board of the stripline filter for viewing the locations of breakdown in the filter. The holes were concentrated over the element ends, where the highest fields are located. A reference photograph of all the holes was taken with an oscilloscope camera, with the viewing door opened. The light due to arcing was photographed with the camera door closed. The arcs were then located by

F15 schematic: marks indicate arc locations at each experimental high-power input

Table shows power levels associated with each arc location

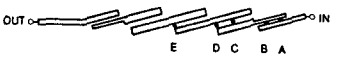

Arc location	Power level (kW)
B	4
A, B, E	40
A, B, C, E,	50
A, B, C, D, E	60

FIGURE 3 Breakdown locations for each peak — pulse level for filter F15.

overlaying the two photos. Each breakdown location and associated input power for filter F15 is shown in figure 3.

PARALLEL-COUPLED STRIPLINE FILTER MODELS

Models were constructed for two of the parallel-coupled stripline filters (F12 and F15), and tuned to the S-parameter data using the microwave analysis computer program called TOUCHSTONE. TOUCHSTONE's optimization feature was used to conform the models to the network analyzer passband data for the filters. High-power models for both filters were developed by adding conducting paths to represent the breakdown between line elements observed during the arc-detection experiments.

The filter dimensions were determined within a tolerance of several mils by x-ray photography. The dielectric constant of the substrate was known a priori. The only unknown parameters in the models were the effective shunt capacitances at the element ends due to the high-electric-flux density produced by the sharp element corners. Values of these capacitances for both filters were found to be on the order of one-hundredth of a picofarad.

Optimization of the filter models mainly involved the variation of these end-capacitance parameters. The correlation between the models and the data was optimized at frequencies between the 30-dB isolation levels of the passband skirts. These frequencies are below the region where the spurious effects of waveguide (TE) mode propagation dominate the filter responses.

The network analyzer measurements were made with a resolution of 50 MHz. The filter models are compared with these data at this resolution. Figure 4 shows this comparison for filter F15. The 3-dB passband frequencies of both filter models are within two percent of those indicated by the low-power data.

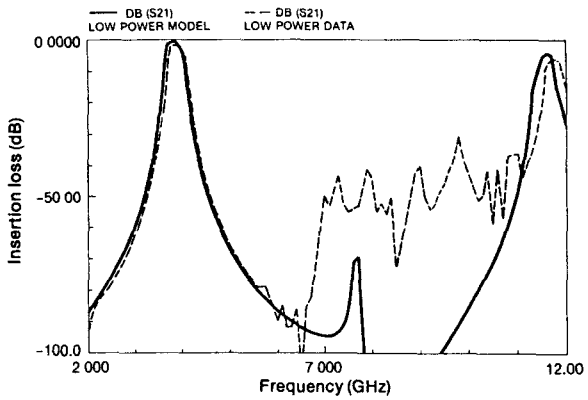

Figure 4 Comparison of low-power model and low-power data for filter F15

The high-power models were constructed with the assumption that after breakdown occurs the arcs can be represented linearly, as perfectly conducting shorts. Only one breakdown mode was observed for filter F12 at high power. The high-power model predicts 59-dB loss at the source frequency (3.28 GHz), in excellent agreement with the experimental values. At 11-kW incident peak power, 0.017-W output was observed, indicating 58-dB isolation. At 43-kW incident peak power 0.04-W output was measured, down 60 dB from the input. The observed high power isolation remains roughly constant at all power levels, supporting the existence of only one breakdown mode for F12.

Multiple breakdown modes were observed for F15. The three modes occur at successively higher power levels, as shown in figure 3. They are characterized by arcing across one, two, and three line-gaps, respectively. The transmission responses from 2 to 12 GHz of each breakdown model for F15 are shown, along with the low-power model, in figure 5. The experimental source frequency is indicated on the plot.

At the source frequency, the one short model predicts 42-dB isolation, 7 dB less than for the low-power model. The data for experimental input levels of 4 to 40 kW indicate 36-dB isolation at 11-kW incident peak power. (The single-arc mode was observed at this input level.) At 17- and 26-kW input, 30-dB isolation was observed. Between 40 and 50 kW, arcing was observed between two line-gaps in filter F15. The transient response for the 43-kW input level (fig. 1b) indicates 77-W output, or 27-dB isolation. The two-arc high power model predicts 25-dB loss at the source frequency. At 60-kW incident peak power, breakdown occurred at three line-gaps in F15. However, no quantitative data were recorded for this case. The three-arc model predicts 17-dB insertion loss at the source frequency.

The high-power models suggest that the degradation of the filter isolation due to breakdown is overshadowed by the mode propagation at X-band and above. However, the high-power model for filter F12 indicates that the isolation is reduced by roughly 50 dB at the passband edges. The high-power model for F15 (fig. 5) shows the progressive degradation of the filter isolation as arcing increases. The two-arc response shows a minimum of 10-dB insertion loss at about 3 GHz, where the low-power filter isolation is almost 50-dB. According to the models, the isolation of the filters is degraded most at the respective passband edges.

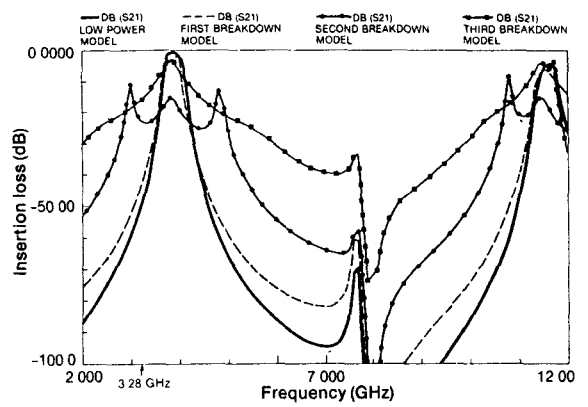

FIGURE 5 Comparison of low-power model with high-power models for filter F15.

RESPONSES OF OTHER FILTER TYPES

High-power experiments with microsecond S-band pulses were performed on a sample of five lumped-element filters. Three of these are low-pass, with cutoff frequencies of about 85 MHz, and are denoted A2, A3, and A4. The other filters tested are denoted B1 and

B2, with a bandpass (Fo = 162 MHz) and a low-pass Fc = 90 MHz) response, respectively.

Table 1 Data for five lumped-element filters

Filter	Arcing	Peak incident power	Incident energy (mJ)	Peak transmitted power	Transmitted energy	Insertion loss (dB)	Low-power loss at source frequency (dB)
A2	Shunt	12.5 kW	12.5	Below noise	--	60+	25
A3	None	34 kW	34	Below noise	--	60+	40
A4	None	9.5 kW	9 5	480 W	0.48 mJ	13	20
	Shunt	24 kW	24	900 W	0.5 mJ	14	20
B1	None	360 W	0 36	6 mW	5 4 nJ	48	65
	Shunt	600 W	0 60	1 2 mW	0.8 nJ	57	65
	Shunt, series	19 kW	19	1 2 mW	2.2 nJ	72	65
B2	None	12 kW	12	800 W	0 32 mJ	11.8	11
	Shunt	18 kW	18	840 W	0.13 mJ	13.3	11
	Shunt	30 kW	30	1.7 kW	0.052 mJ	12.5	11

Table 1 gives the high-power experimental results for the lumped filters, including observed breakdown. The incident power is in the form of 1 μs pulses, at 2.74 GHz. Note that all arcing observed for the lumped filters was to ground (except for the 19-kW response of B1, which exhibited series arcing after shunt breakdown). Upon shunt breakdown, all or part of the remaining pulse is reflected, resulting in increased isolation. The responses of these filters were therefore characterized by tail-biting, whereby the back end of the output pulse is suppressed and the transmitted energy reduced. As a result, incident microwave pulses did not degrade lumped-element filter isolation to peak powers over 30 kW.

Experiments were also conducted with the 2.74-GHz pulsed source on two other filters, denoted S1 and S2. S1 is a bandpass filter in microstrip, consisting of a low-pass stepped impedance section followed by a high-pass section with series-coupled capacitive gaps (a video detector is built into S1). The stepped-impedance structure consists of a center conducting strip which has alternately wide and narrow sections. The center conductor sits over a ground plane, separated by dielectric substrate. The wide sections act as shunt capacitors, while the narrow sections act as series inductors, thus forming a low pass filter. The other filter, S2, has a resonant interdigital structure. This consists of a row of conductive posts protruding from one wall of the filter to the other (ground) wall, with tiny air gaps at varying points between the walls.

The interdigital structure of S2 was not susceptible up through 52-kW incident peak power. The narrowest gaps in this interdigital structure are between the resonant posts and the ground wall, so that breakdown, if any, should occur in shunt. The microstrip filter, S1, did not arc at 870-W input, and the isolation was 61 dB. However, at 1.3-kW input series arcing began after 150 ns, lowering the isolation to 49 dB. At 3.6 kW, series arcing began almost immediately (50 ns), followed 200 ns later by shunt arcing.

All breakdown observed in S1 is probably taking place in the high-pass section of the filter. This latter section is far more susceptible than the preceding stepped-impedance section, owing to its tiny air-gap elements. The series breakdown that occurs in S3 is due to arcing across series air gaps, while the subsequent shunt arcing takes place across shunt tuning-gaps. The energy allowed through the filter is limited by the shunt breakdown. Although the low-pass section is nearest the input of S1, no stepped impedance breakdown was observed in experiments with incident peak power to over 52 kW.

CONCLUSIONS

This study is concerned with identifying worst-case results of microwave energy coupled into electronic systems. Most filter types (and all connectors) arc to ground much more readily than in series, therefore giving added isolation and protecting subsequent circuit components. However, since filters with series air gaps tend to allow increased energy through upon breakdown, they have been the focus of most of our attention. An innovative method of observing specific arc locations in parallel-coupled stripline filters was accomplished using a conventional oscilloscope camera. This information was used to develop models of the parallel coupled-stripline filters. These models are in good agreement with the low-power S-parameter data from network analyzer measurements made on the filters. High-power models were constructed using zero impedance paths to represent arcs. These models extend limited high-power data, giving the wideband responses of the parallel-coupled stripline filters under conditions of breakdown.

REFERENCES

1. Alexander D. MacDonald, Microwave Breakdown in Gases, Wiley, N.Y., New York (1966).